


FULL PAPER

Open Access



Tensile overpressure compartments on low-angle thrust faults

Richard H. Sibson* 

Abstract

Hydrothermal extension veins form by hydraulic fracturing under triaxial stress (principal compressive stresses, $\sigma_1 > \sigma_2 > \sigma_3$) when the pore-fluid pressure, P_f , exceeds the least compressive stress by the rock's tensile strength. Such veins form perpendicular to σ_3 , their incremental precipitation from hydrothermal fluid often reflected in 'crack-seal' textures, demonstrating that the tensile overpressure state, $\sigma_3' = (\sigma_3 - P_f) < 0$, was repeatedly met. Systematic arrays of extension veins develop locally in both sub-metamorphic and metamorphic assemblages defining *tensile overpressure compartments* where at some time $P_f > \sigma_3$. In compressional regimes ($\sigma_v = \sigma_3$), subhorizontal extension veins may develop over vertical intervals < 1 km or so below low-permeability sealing horizons with tensile strengths $10 < T_o < 20$ MPa. This is borne out by natural vein arrays. For a low-angle thrust, the vertical interval where the tensile overpressure state obtains may continue down-dip over distances of several kilometres in some instances. The overpressure condition for hydraulic fracturing is comparable to that needed for frictional reshear of a thrust fault lying close to the maximum compression, σ_1 . Under these circumstances, especially where the shear zone material has varying competence (tensile strength), affecting the failure mode, dilatant fault–fracture mesh structures may develop throughout a tabular rock volume. Evidence for the existence of fault–fracture meshes around low-angle thrusts comes from exhumed ancient structures and from active structures. In the case of megathrust ruptures along subduction interfaces, force balance analyses, lack of evidence for shear heating, and evidence of total shear stress release during earthquakes suggest the interfaces are extremely weak ($\tau < 40$ MPa), consistent with weakening by near-lithostatically overpressured fluids. Portions of the subduction interface, especially towards the down-dip termination of the seismogenic megathrust, are prone to episodes of slow-slip, non-volcanic tremor, low-frequency earthquakes, very-low-frequency earthquakes, etc., attributable to the activation of tabular fault–fracture meshes at low σ_3' around the thrust interface. Containment of near-lithostatic overpressures in such settings is precarious, fluid loss curtailing mesh activity.

Introduction

Material properties aside, the formation and reactivation of brittle faults and fractures is largely governed by the triaxial stress state within the rock mass and by the pore-fluid pressure, P_f , within the rock mass (Hubbert and Rubey 1959; Jaeger and Cook 1979). Recognizing the boundary condition of zero shear stress along the Earth's free surface (taken as horizontal), Anderson (1905) postulated the existence of three basic stress regimes in the crust depending which of the principal compressive stresses ($\sigma_1 > \sigma_2 > \sigma_3$) coincides with the vertical stress,

σ_v . Normal faulting prevails where the crust is under extension with $\sigma_v = \sigma_1$; strike-slip faulting occurs where $\sigma_v = \sigma_2$; and thrust faulting develops where the crust is shortening under horizontal compression with $\sigma_v = \sigma_3$. Information from borehole measurements (Townend and Zoback 2001), earthquake focal mechanisms (Célérier 2008), and palaeostress inversions (Lisle et al. 2006) demonstrates that 'Andersonian' stress states (one principal stress vertical and the other two horizontal) prevail over large areas of continental and oceanic crust (Zoback 1992). These 'Andersonian' stress orientations provide useful reference states for general consideration, though significant departures undoubtedly occur. For example, although a subduction interface shear zone (SISZ)

*Correspondence: rick.sibson@otago.ac.nz
Department of Geology, University of Otago, Dunedin 9054, New Zealand

is, in essence, a large-scale thrust fault accommodating underthrusting of oceanic lithosphere, significant departures from vertical and horizontal stress trajectories are expected from: (1) the kinematic control exerted by a weak plate boundary shear zone; (2) force balance analyses associated with a tapering accretionary wedge (e.g. Dahlen 1990); and (3) time variations in the stress field as a consequence of stress cycling associated with intermittent megathrust rupturing along the SISZ (Hasegawa et al. 2012).

Hubbert and Rubey (1959) were the first to apply the simple principle of effective stress to rocks whereby pore-fluid pressure reduces all normal stresses to 'effective' values, $\sigma_n' = (\sigma_n - P_f)$, suggesting also that fluid overpressures were a means of reducing basal friction allowing emplacement of thrust sheets along low-angle overthrusts. They also defined a pore-fluid factor, $\lambda_v = P_f/\sigma_v$, usefully relating the level of pore-fluid pressure with respect to the vertical stress. Where fluid pressure, P_f , in pore and/or fracture space is freely interconnected up to a water table at the earth's surface, the pore-fluid pressure is hydrostatic ($\lambda_v \sim 0.4$). Pore-fluids are overpressured wherever pore-fluid pressures exceed hydrostatic values (i.e. $\lambda_v > 0.4$). Fluid at a depth, z , is overpressured towards lithostatic values ($\lambda_v \rightarrow 1.0$) when P_f approaches the lithostatic load ($\sigma_v = \rho g z$, where ρ is average rock density and g the gravitational acceleration). Supralithostatic overpressures ($\lambda_v > 1.0$) occur where $P_f > \sigma_v$.

Formation and opening of extension fractures perpendicular to least compressive stress, σ_3 , in intact rock occurs by hydraulic fracturing when

$$P_f = \sigma_3 + T_0 \quad (1)$$

where T_0 is rock tensile strength, provided $(\sigma_1 - \sigma_3) < 4 T_0$ inhibiting shear failure of the rock (Secor 1965; Etheridge 1983). For competent sedimentary rocks and crystalline rocks with $T_0 \sim 10$ MPa and ~ 20 MPa, respectively (Lockner 1995), differential stresses are restricted to < 40 and < 80 MPa. A local absence of existing fractures suitably oriented for shear reactivation is also a prerequisite. The *tensile overpressure state* ($P_f > \sigma_3$) thus defines portions of the rock mass with the potential for hydraulic fracturing leading to the formation of extension vein arrays.

In compressional settings where $\sigma_v = \sigma_3$, the *tensile overpressure state* ($P_f > \sigma_3$) equates to the maximum sustainable overpressure and is close to lithostatic (Sibson 2003). It is conducive to the development and fluid activation of dilatant fault–fracture meshes developed in tabular rock volumes around low-angle thrusts and may be responsible for the range of time-dependent slow-slip activity observed around such structures.

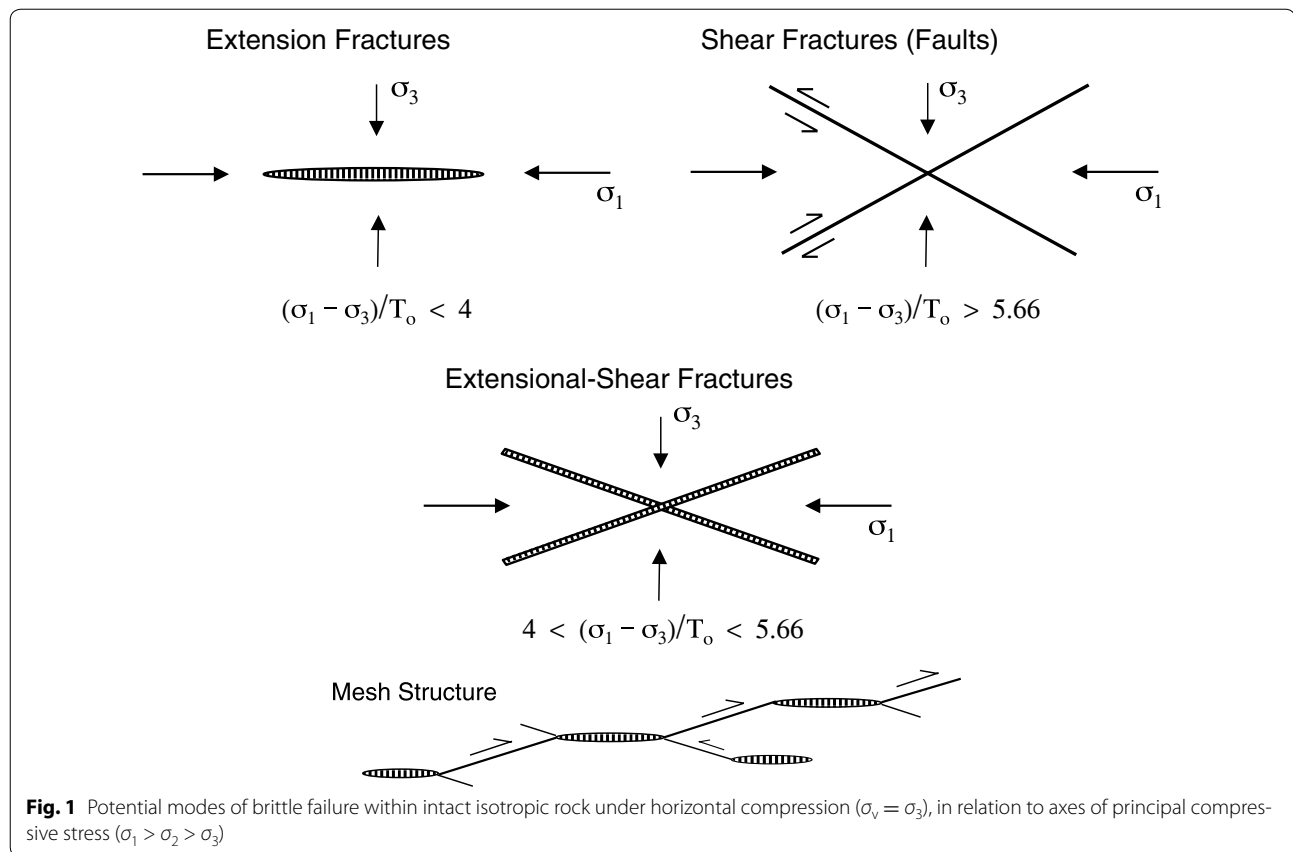
Controls on brittle failure of rock

Criteria for all modes of brittle failure in rock include the levels of differential stress and pore-fluid pressure [through the principle of effective stress, $\sigma_n' = (\sigma_n - P_f)$]. The two drivers to failure, therefore, are $(\sigma_1 - \sigma_3)$ and P_f , which may act separately or together. In 'classical' rock mechanics (e.g. Secor 1965; Jaeger and Cook 1979; Sibson 2000), the composite Griffith–Coulomb failure curve for intact rock in τ/σ_n' space can be normalized to nominal rock tensile strength, T_0 (half the cohesive strength). The ratio of differential stress to rock tensile strength $(\sigma_1 - \sigma_3)/T_0$ then determines the potential mode of brittle failure (Fig. 1). For 'generic' internal friction, $\mu_i = 0.75$ in the compressional field, extension fractures form only when $(\sigma_1 - \sigma_3)/T_0 < 4$, hybrid extensional-shear fractures require $4 < (\sigma_1 - \sigma_3)/T_0 < 5.66$, and compressional shear fractures (faults) form when $(\sigma_1 - \sigma_3)/T_0 > 5.66$ (Secor 1965). Additionally, as noted above, the presence of existing fractures appropriately oriented for reshear within the stress field suppresses the formation of any new extensional or hybrid extensional-shear fractures. Fluid circulation through a fractured rock mass may, however, restore cohesive and tensile strength by hydrothermal cementation (e.g. silicification), effectively restoring 'intact' character.

Hydraulic extension fracturing can thus only be induced: (a) within intact rock in the absence of cohesionless faults suitably oriented for shear reactivation; (b) in settings where existing fractures are severely misoriented for reshear (containing the σ_2 axis and lying at $> c. 60^\circ$ to σ_1); and (c) where existing fractures have regained cohesive strength through hydrothermal cementation, etc. Rock tensile strength is thus critical in determining whether rock fails in tension or in shear under increased fluid pressure. Under the same differential stress, fluid-induced failure in heterogeneous material of mixed competence (differing tensile strength) may therefore give rise to mixed-mode brittle failure with volumetric fault–fracture meshes comprising interlinked shear and extensional fractures distributed throughout the rock mass (Sibson 1996, 2000).

Tensile overpressure compartments

Extension veins [often with 'crack-seal' infillings of quartz, calcite, etc., reflecting incremental precipitation (Ramsay 1980)] thus diagnose the *tensile overpressure state* ($\sigma_3' = (\sigma_3 - P_f) < 0$, or $P_f > \sigma_3$) once having been achieved within the rock mass. In extensional ($\sigma_v = \sigma_1$) and strike-slip ($\sigma_v = \sigma_2$) stress regimes where σ_3 is horizontal, vertical extension veins may form under hydrostatic levels of fluid pressures in the near-surface ($z < 1\text{--}2$ km), but suprahydrostatic fluid pressures are required for their formation at depths more than a



kilometre or so (Secor 1965). In compressional regimes ($\sigma_v = \sigma_3$), however, supralithostatic overpressures are required at all depths for the formation of subhorizontal extension veins unless significant stress heterogeneity exists such that $\sigma_v < \sigma_3$. Systematic arrays of hydrothermal extension veins are widely developed in both subgreenschist and greenschist metamorphic assemblages (e.g. Fig. 2) and can be used to define former *tensile overpressure compartments* where $P_f > \sigma_3$.

Compressional stress regimes ($\sigma_v = \sigma_3$) are particularly effective at containing fluid overpressure because: (1) activated faults and fracture tend to be flat-lying, inhibiting vertical flow and (2) under the same differential stress, faults and fractures in compressional regimes are generally capable of sustaining higher overpressures before activation to provide drainage paths than in other tectonic regimes (Sibson 2003). As with compartmentalized overpressures developed in sedimentary basins (Hunt 1990), development of overpressure generally requires a low-permeability sealing horizon perhaps associated with silicification or some other form of hydrothermal cementation. If the sealing horizon has a tensile strength, T_s , overpressure will increase across it to a maximum value, $P_f = \sigma_3 + T_s$, at its base, where hydrofractures

form, below which, provided pore/fracture space is interconnected, the pressure gradient reverts to hydrostatic (Sibson and Scott 1998). The supralithostatic overpressure condition, $P_f > \sigma_v$, will be maintained below the base of the seal over a vertical interval:

$$\Delta z = T_s / (\rho - \rho_f)g \quad (2)$$

(where ρ is rock density, ρ_f is fluid density, and g is gravitational acceleration) to a depth where the pore-fluid pressure drops below lithostatic.

Vertical and lateral extent of tensile overpressure compartments

Variations in rock tensile strength allow horizontal hydrofracturing throughout the vertical interval of supralithostatic overpressure (Fig. 3). Sealing horizons may also migrate vertically with time. Tensile rock strength ranges from 1 to 10 MPa for sedimentary rocks of low to moderate competence, to 20 MPa or so for high-competence crystalline rocks (Lockner 1995). For $T_s = 10$ –20 MPa, $\Delta z = 600$ –1200 m. These values compare with the vertical extent of horizontal vein arrays observed in Panasqueira Mine, Portugal (Foxford et al. 2000) and Sigma Mine, Val d'Or (Robert and Brown 1986). If the seal to a tensile

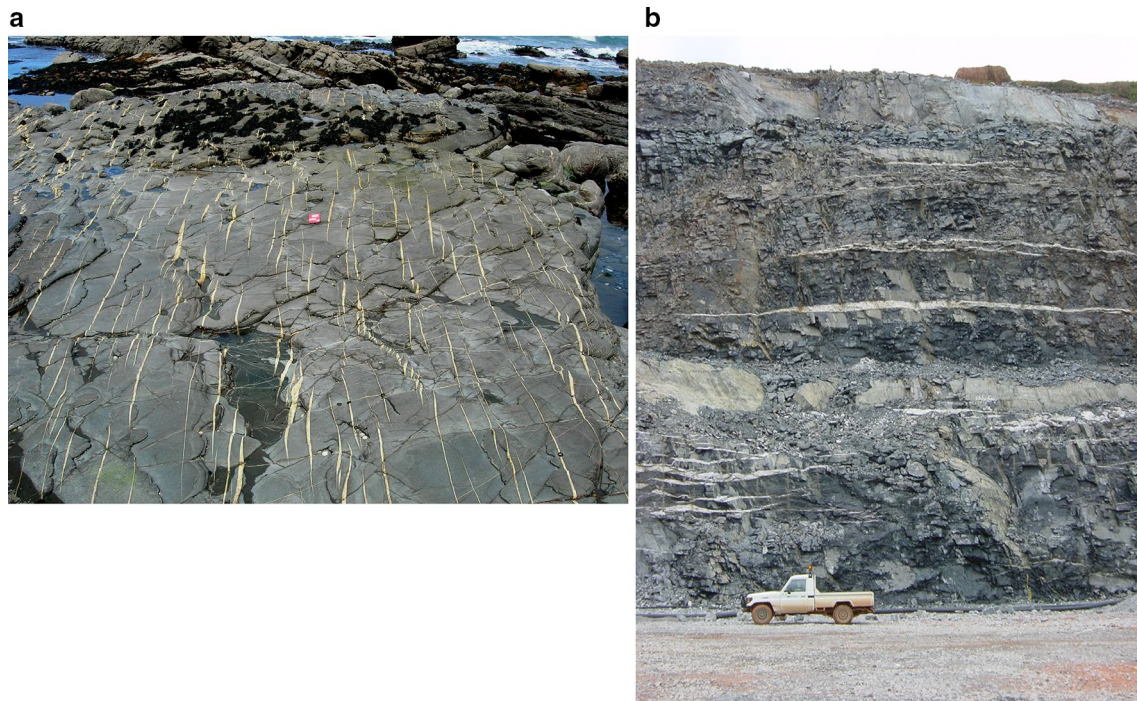


Fig. 2 Systematic arrays of hydrothermal extension veins: **a** quartz vein array infilling subvertical extension fractures in Carboniferous sandstone (strike-slip regime), Millook, North Devon; **b** array of subhorizontal gold-bearing quartz veins, Damang Mine, Ghana (Tunks et al. 2004; photograph courtesy Andrew Tunks)

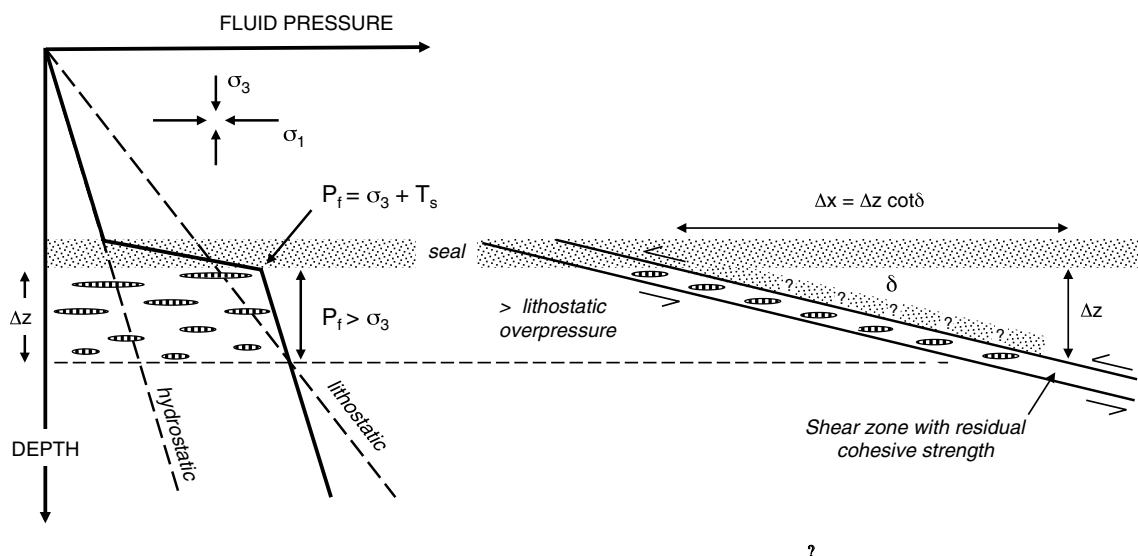


Fig. 3 Vertical and lateral extent of hydrofracture arrays below a sealing horizon in a compressional stress regime. Potential hanging-wall seal discussed in text indicated by *dashed shading*

overpressure compartment extends across a low-angle thrust-sense shear zone with dip, δ (perhaps retaining low cohesive strength through hydrothermal cementation—Fig. 3), the tensile overpressure compartment may extend

laterally for a distance, $L = \cot \delta \Delta z$. For $\Delta z = 1$ km and $\delta = 10^\circ, 5^\circ$, and 1° , $L = 5.7, 11.4$, and 57 km, respectively. Tensile overpressure compartments may thus extend laterally for considerable distances around low-dipping

thrust faults that have regained some cohesion. In reality the permeability structure is likely to be more complex than that pictured in Fig. 3. Upward flow of overpressured fluids along a thrust (cf. Saffer and Tobin 2011) is likely to transport solutes derived from deformation involving pressure solution within fine-grained fault rocks as well as solutes from prograde metamorphism of the footwall—all may contribute to cementation (especially silicification) of the hanging wall.

Fault–fracture meshes in compressional regimes

Dispersed fault–fracture meshes may develop in compressional regimes in a number of configurations (Fig. 4). Possibilities to be considered include: (1) refraction of thrust faults across competence layering (e.g. bedding) creating localized sites of dilatation [factors affecting the degree of fault refraction across competence boundaries are discussed by Ferrill and Morris (2003)]—the overall dip envelope then depends on the ratio of extension fractures to thrust-sense shear fractures; (2) dilational thrust stepovers/jogs arising from stress heterogeneity associated with en echelon thrust segmentation; (3) distributed fault–fracture meshes developing within a mixed competence *mélange* shear zone (Sibson 1996; Fagereng and Sibson 2010). To a greater or a lesser extent, fault–fracture meshes occupy a substantial rock volume rather than

being restricted to discrete planar slip zones. An important issue (not further considered) is whether dilatation accompanying opening of extension fractures and their infilling with precipitates is compensated in the long run by volume loss in the surrounding rock mass from dissolution and solution transfer.

Frictional reshear of low-angle thrusts

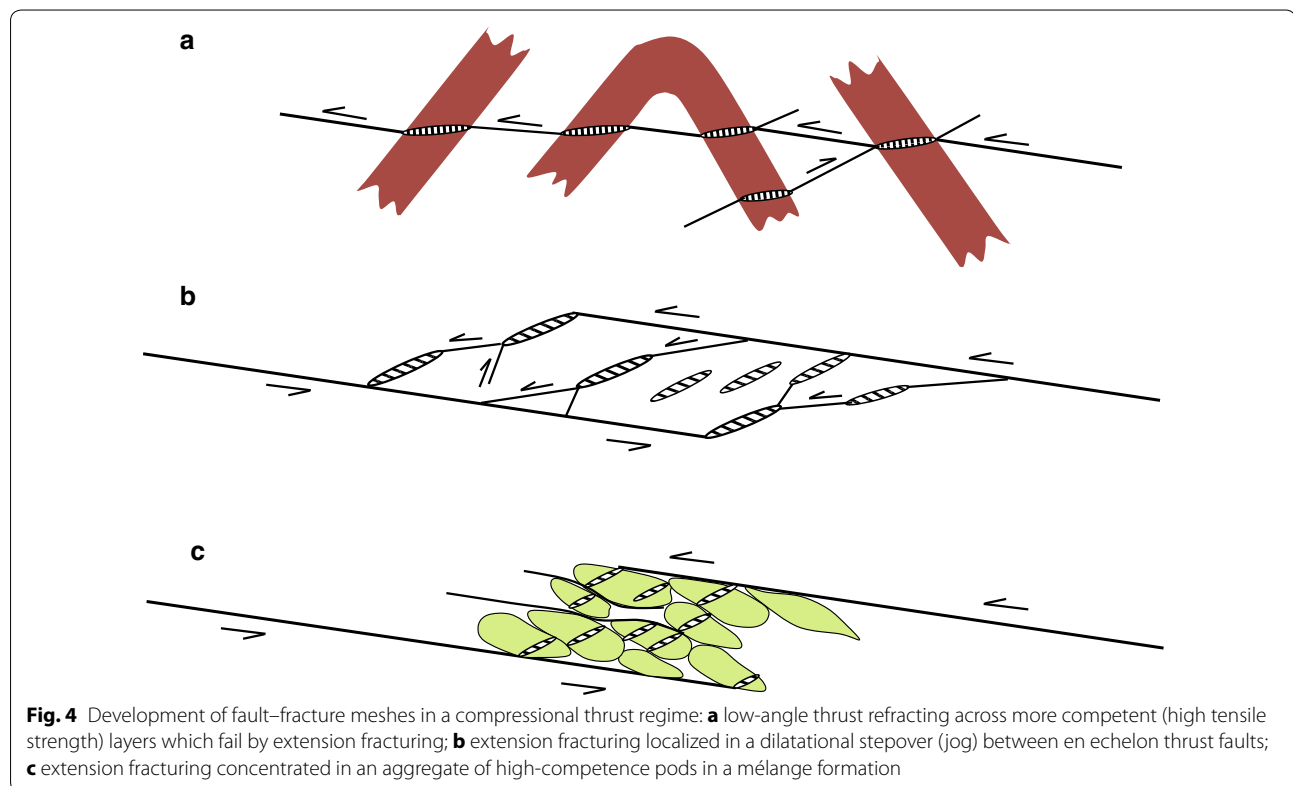
In a simple compressional regime with $\sigma_v = \sigma_3$, a low-dipping planar discontinuity (e.g. an existing fracture or fault, a bedding plane, or foliation) may lie at a very low angle to σ_1 . The stress condition for frictional reactivation of an existing cohesionless plane with a friction coefficient, μ_s , containing the σ_2 axis is:

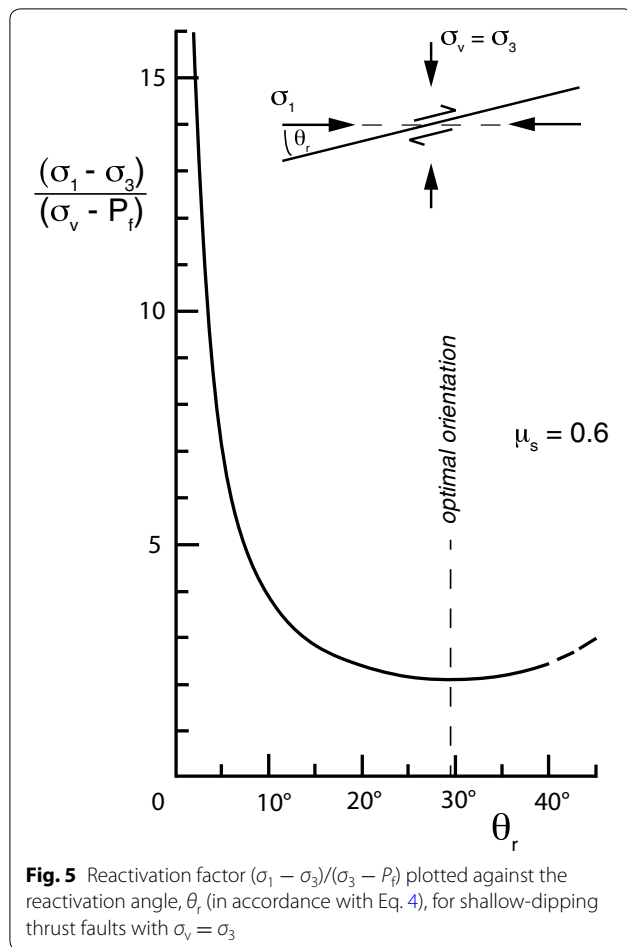
$$\begin{aligned} \sigma'_1/\sigma'_3 &= (\sigma_1 - P_f)/(\sigma_3 - P_f) \\ &= (1 + \mu_s \cot \theta_r)/(1 - \mu_s \tan \theta_r) \end{aligned} \quad (3)$$

where θ_r is the angle of reactivation with respect to σ_1 (Sibson 1985). For the situation where $\sigma_v = \sigma_3$, this expression may be rewritten as:

$$\begin{aligned} (\sigma_1 - \sigma_3)/(\sigma_3 - P_f) &= (\sigma_1 - \sigma_3)/(\sigma_v - P_f) \\ &= \mu_s[(\tan \theta_r + \cot \theta_r)/(1 - \mu_s \tan \theta_r)] \end{aligned} \quad (4)$$

defining the reactivation condition plotted in Fig. 5 for $\mu_s = 0.6$ [the lower end of Byerlee's (1978) range for





hard-rock friction]. The ratio $(\sigma_1 - \sigma_3)/(\sigma_v - P_f) \rightarrow \infty$ as $\theta_r \rightarrow 59^\circ$ or 0° , requiring $P_f \rightarrow \sigma_v$. In the case of a thrust fault that retains (or has acquired) some cohesive strength, c , the fluid pressure requirement for reactivation of faults approaching frictional lock-up becomes supralithostatic ($P_f = \sigma_v + c/\mu_s$) (Sibson 2009). The essential point is that the overpressure condition needed to induce thrust reshear along thrusts at very low angles to σ_1 ($P_f \rightarrow \sigma_v$) is near-lithostatic or even supralithostatic and very close to the hydraulic fracturing criterion. Under such circumstances, slight heterogeneities in the stress field or in rock material properties may allow hydraulic extension veins to form subparallel to thrust-reactivated planes.

Tensile overpressure compartments along low-angle intracontinental thrusts

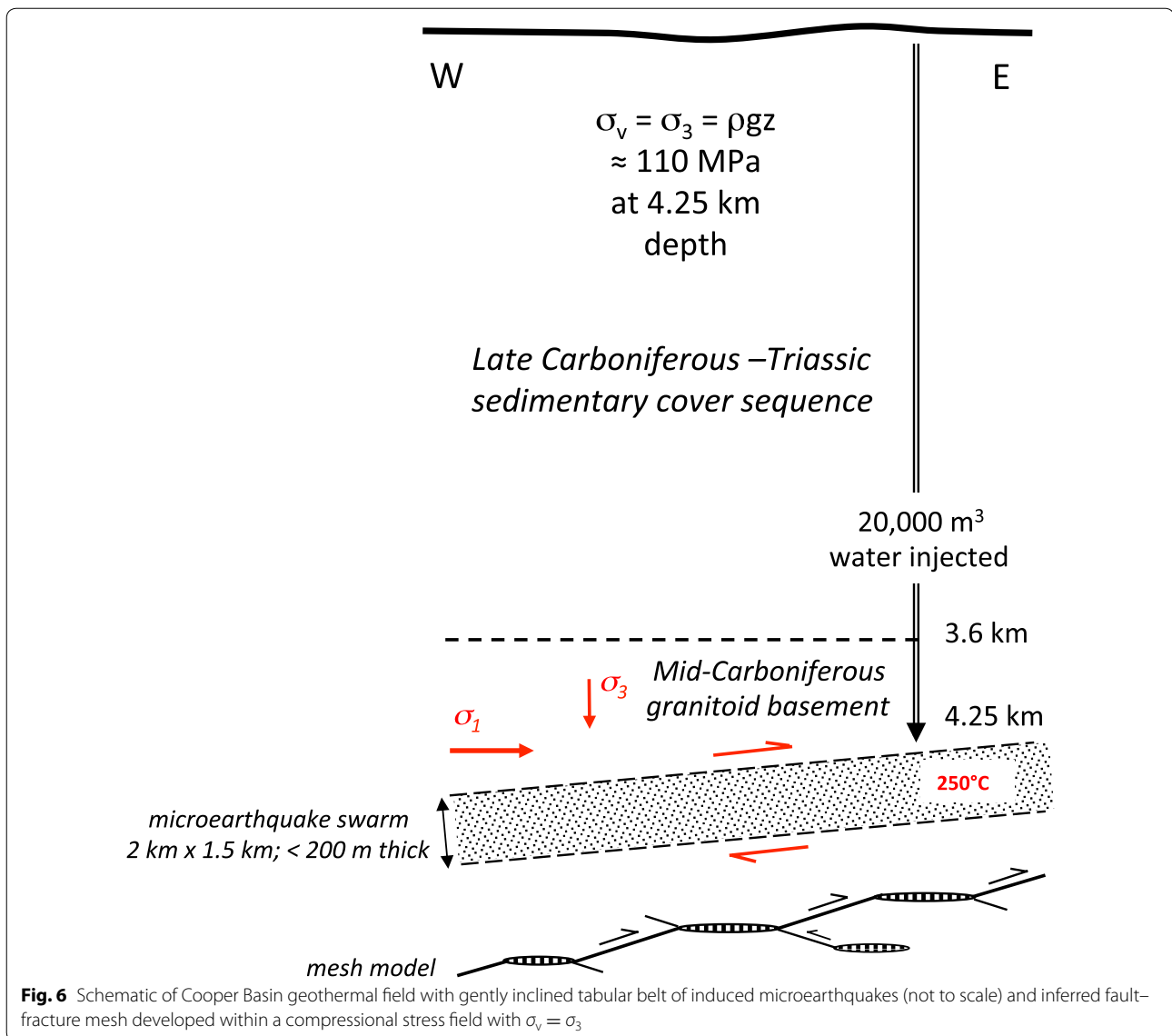
Here we consider geological and geophysical evidence supporting the existence of tensile overpressure compartments associated with both active and ancient low-angle thrust faults developed within continental settings.

San Gabriel Mountains bright reflective zone

The LARSE seismic line (Ryberg and Fuis 1998; Fuis et al. 2001) runs NNE-NE from Seal Beach across the Los Angeles Basin, then crosses the upthrust crystalline massif of the San Gabriel Mountains and the bounding San Andreas fault to the Mojave Desert. The San Gabriel Mountains are made up of Proterozoic age gneisses with a metamorphosed cover sequence intruded by Mesozoic granitoid plutons, all thrust over the Pelona Schist along the Vincent thrust fault. The experiment revealed the existence of a bright reflective zone below the San Gabriel Mountains with two particularly intense bright-spots, deepening from 18 km in the SW to 23 km in the NE (average dip c. 10°), more or less coincident with the base of the seismogenic zone. Recognition of a marked negative velocity step at the top of the c. 500-m-thick low-velocity zone has led to its interpretation as a lithostatically overpressured thrust-sense ductile shear zone serving as a mid-crustal décollement. Arrays of gaping flat-lying macroscopic cracks infilled with lithostatically pressured fluid and lying subparallel to shear zone foliation are inferred to account for the markedly high reflectivity of the shear zone (Ryberg and Fuis 1998).

Cooper Basin induced microearthquake swarm

The Cooper Basin in north-eastern South Australia contains a cover sequence of Late Carboniferous–Triassic sediments, some 3.6 km thick, overlying a mid-Carboniferous granitic basement. The contemporary stress regime is one of regional compression with σ_3 vertical and regional σ_1 oriented $082^\circ \pm 5^\circ$ (Holl and Barton 2015). The basement assemblage below the insulating blanket of cover sediments is a significant source of radiogenic heat, and the region has been assessed as an enhanced geothermal system (EGS) with a temperature of c. 250°C encountered at the base of a borehole some 4.25 km deep (Baisch et al. 2006). A series of injection experiments down different wells produced a tabular, flat-lying microearthquake swarm <100–150 m thick extending initially over an area of $2\text{ km} \times 1.5\text{ km}$, but expanding significantly with further injection experiments (Baisch et al. 2009, 2015; Cox 2016), and dipping very gently WSW (Fig. 6). Of the 525 focal mechanisms obtained from the induced microearthquake swarm, the great majority yield thrust solutions with one very low-angle nodal plane dipping c. 10° W parallel to the sheet dip of the swarm, but a few have more moderately dipping nodal planes (Baisch et al. 2015). Fluid pressure during injection at the bottom of the wells approached lithostatic or slightly supralithostatic (Holl and Barton 2015). The activated structure hosting the swarm is generally interpreted as a simple planar thrust fault, but the volumetric character of the swarm, together with its very low-angle attitude, suggests

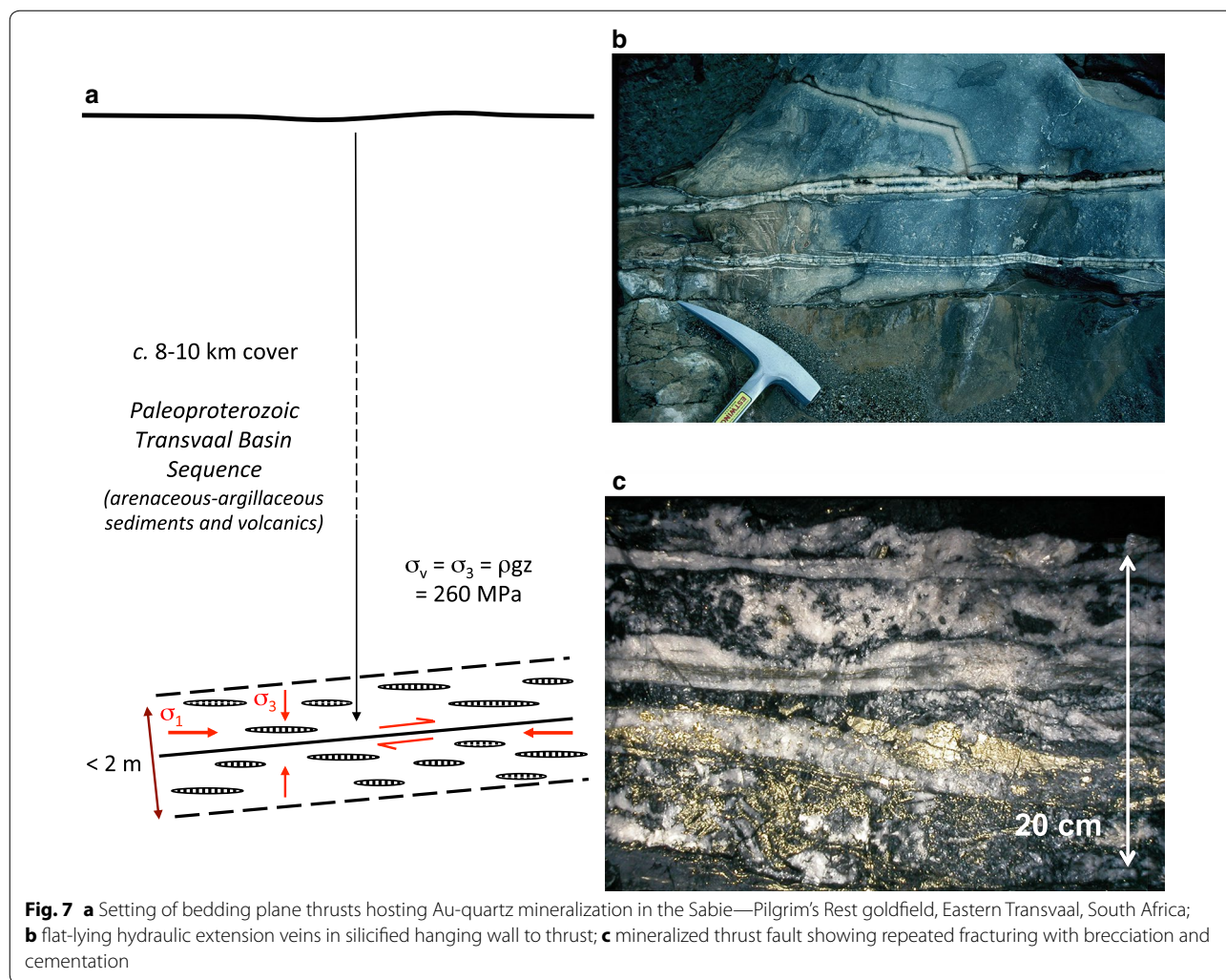


it may represent a distributed fault–fracture mesh (Sibson 1996) comprising interlinked minor thrusts and extension fractures developed by hydrofracturing (Fig. 6). Note that this swarm was induced by comparatively rapid overpressuring, and the length of time for which overpressuring may be maintained in comparison with natural settings, given the possibility of subcritical crack growth, etc., is questionable. Nonetheless, at the very least the swarm activity provides an example of thrusting activity on low-angle planes almost perpendicular to σ_3 induced by close-to-lithostatic fluid overpressures.

Sabie—Pilgrim’s Rest Au-quartz mineralization

The Sabie—Pilgrim’s Rest goldfield of the Eastern Transvaal in South Africa is hosted within the lower Transvaal

carbonate-siliciclastic sequence exposed along the westerly dipping rim of the Palaeoproterozoic Transvaal Basin (Harley and Charlesworth 1992, 1996). Au-quartz mineralization is largely hosted along bedding plane thrusts and is likely coeval with early stages of the emplacement of the Bushveld igneous complex (c. 2060 Ma) (Boer et al. 1995). In the Elandshoogte Mine, thin (0.2–0.5 m, locally <2 m) zones of laminated, incrementally deposited Au-quartz mineralization resulting from multiple episodes of brecciation and hydrothermal cementation are concentrated along bedding plane thrusts dipping c. 5°W. The mineralized bedding plane shears are sometimes imbricated in thrust duplexes and are also flanked by bands of silicification in which flat-lying extension veins occur subparallel to the bedding plane thrusts (Fig. 7).



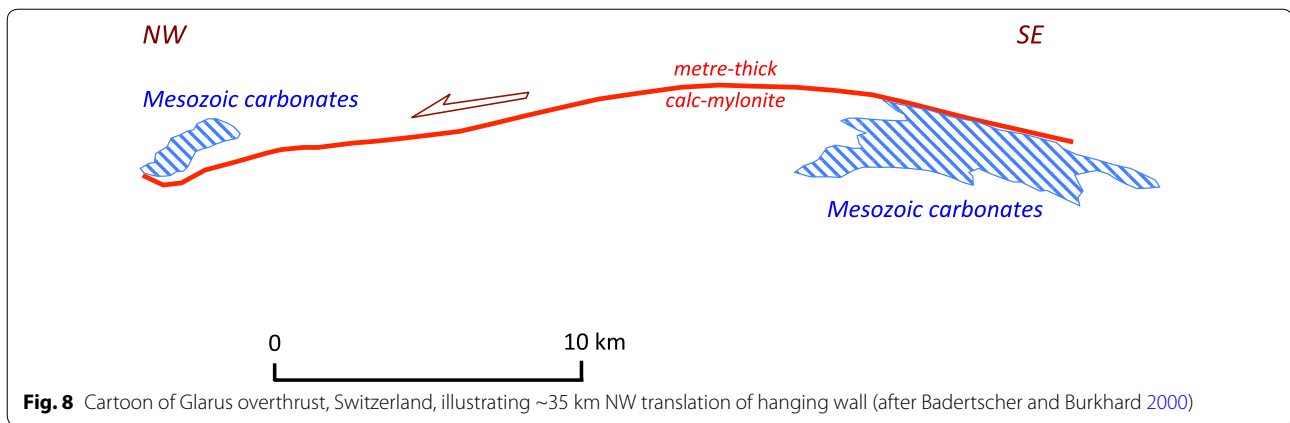
Subordinate steep (sometimes subvertical) leader veins also occur locally throughout the goldfield. Plausibly, they formed from time to time as a consequence of transitory switching to an extensional stress field following total shear stress release along the low-angle thrusts.

The evidence for incremental precipitation coupled with the low transport solubility of gold (c. 10 ppb?) suggests that intermittent high flux episodes of hydrothermal flow passed through the system. Mineralization appears to have developed under a stratigraphic cover of c. 8.2 km (corresponding to an overburden pressure of 220–250 MPa) at a temperature of c. 320 °C, typical of a mesothermal assemblage (Boer et al. 1995). The significance of the vein assemblage occupying bedding plane thrusts with subparallel (within a few degrees) extension veins is the demonstration that thrusting occurred at very close to lithostatic fluid overpressures (Harley and Charlesworth 1996).

Glarus Overthrust, Switzerland

The Glarus Overthrust of Oligocene–Miocene age is well exposed at elevations approaching 3000 m in the Swiss Alps as a generally flat-lying but arched thrust contact (Fig. 8) between overlying Mesozoic carbonates and the Permian Veruccano formation emplaced over Tertiary Flysch (Herwegh et al. 2008). The present flat-lying attitude of the Glarus Thrust differs from its likely low-angle (c. 15°S) orientation when active (Pfiffner 1986). Over 35 km of northward translation has occurred across an ~1-m-thick shear zone of shear zone of highly deformed carbonate—the Lochseiten tectonite—with crystal plastic deformation occurring over temperatures ranging from 230° to 360 °C with increasing palaeodepth.

The Lochseiten calc-mylonite was interpreted by Schmid (1975) as resulting from superplastic deformation. However, more recently Badertscher and Burkhard (2000) documented field, petrographic, and isotopic

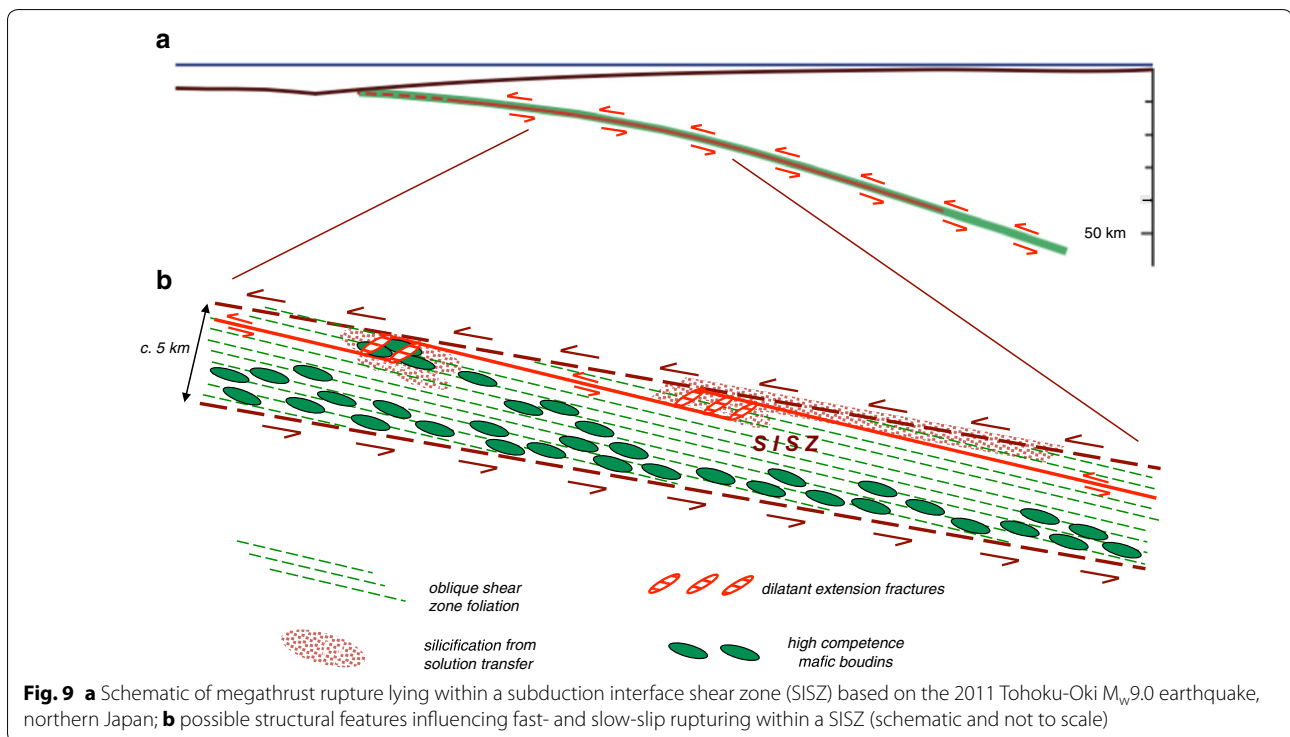


evidence for multiple episodes of cataclasis and hydrofracturing leading to vein formation (indicative of the tensile overpressure state), overprinted by ductile crystal plastic smearing of cataclasites and veins. Most of the calcite in the Lochseitenkalk tectonite thus likely originated as vein calcite. The isotopic evidence suggests that large fluid volumes were channelled along the mylonitic shear zones with periodic build-up of fluid overpressure to near-lithostatic values inducing cataclastic deformation, hydrofracturing and vein formation, followed by renewed crystal plastic deformation once discharge and drops in fluid pressure had occurred.

Similar textures and deformation histories have been invoked for calc-mylonites associated with the Gavarnie Thrust in the Pyrenees (McCaig et al. 1995) and the McConnell Thrust in Alberta (Kennedy and Logan 1997).

Tensile overpressure compartments along subduction interfaces

Megathrust ruptures hosted within subduction interface shear zones (SISZ) (Fig. 9) are also low-angle structures, dipping $<5^\circ$ in the vicinity of the trench inner wall to c. 15° around the maximum down-dip limit of the ruptures at depths of 40 ± 5 km (governed by isotherms in



the 350–450 °C range), perhaps 150–200 km inboard from the trench axis (Hyndman 2007; Lay et al. 2012). Details of the internal structure of SISZ and the physical conditions prevailing therein are inevitably speculative, but are constrained by geophysical observations and the structural characteristics of analogous exhumed thrust zones. Mélange formations so typical of exhumed SISZ (Fagereng 2011; Kimura et al. 2012) are of particular interest because of the likelihood of extreme stress and competence (i.e. tensile strength) heterogeneity within such formations (Fagereng and Sibson 2010).

A strong case can be made that the megathrusts [responsible for >90% global release of seismic moment (Pacheco and Sykes 1992)] are weakened by fluid overpressuring to near-lithostatic values ($\lambda_v \rightarrow 1.0$). The hosting subduction interface shear zones (SISZ) likely contain a mélange assemblage of entrained fluid-rich ocean floor sediments (muds, siliceous oozes, etc.), plus trench wall sediments (turbidite sands and muds) along with similar material from the accretionary prism, together with slivers of oceanic crust and occasional seamount volcanics (Von Huene and Scholl 1991; Kimura et al. 2012). Overpressures within the material entrained in SISZ probably arise through a combination of compaction under increasing mean stress together with metamorphic dehydration of the descending oceanic crust under rising temperature (Saffer and Tobin 2011). Force balance analyses taking account of surface and Moho topography limit depth-averaged shear stress along subduction interfaces to <40 MPa (Wang and Suyehiro 1999; Lamb 2006; Seno 2009), as does the lack of evidence for significant shear heating along the interface (Peacock 2004), and the inference of total shear stress release during large megathrust ruptures (Hasegawa et al. 2012). This equates to an ‘effective friction coefficient’ $\mu\sigma' \approx \mu\sigma(1 - \lambda_v)$ of 0.03 averaged over the full depth (c. 40 km) of the seismogenic megathrust (Sibson 2014). Even for the lowest measured friction coefficients ($\mu\sigma \sim 0.1$ for saponite-rich gouge) overpressures with $\lambda_v > 0.7$ are required to match this effective friction coefficient.

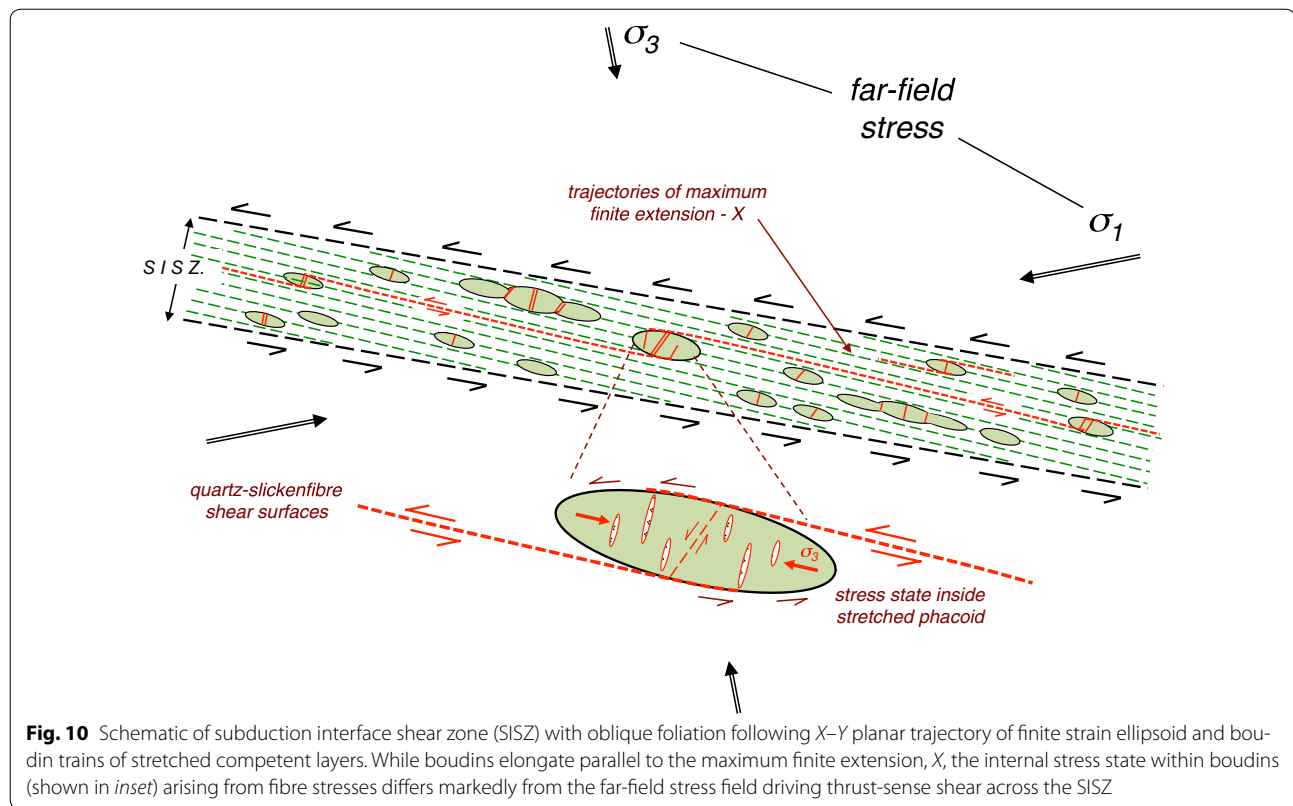
These inferences are supported by geophysical imaging which reveals thin (several km scale) tabular shear zones, locally highly reflective and with anomalously low V_p , high V_p/V_s and low Q (e.g. Kodaira et al. 2002; Abers 2005; Eberhardt-Phillips and Reyners 1999; Song et al. 2009) thought to represent fluid-rich low-permeability SISZ. In a profile across the Costa Rica subduction margin, Bangs et al. (2015) found a high-reflectivity interface extending to depths of c. 6 km, implying an overpressured fluid-rich interface drained by arrays of fluid-rich faults cutting through the hanging wall. MT electrical imaging provides additional constraints on fluid content. For instance, the seismogenic portion of the Cascadia

subduction interface below Vancouver Island coincides with an inclined tabular zone of high electrical conductivity (Kurtz et al. 1990; Soyer and Unsworth 2006). In southwest Japan, likewise, a highly reflective low-velocity layer dips c. 7°NW below Shikoku Island, down-dip from a subducting seamount on the inner wall of the Nankai Trough, defining the subduction interface that ruptured in the 1946 M_w 8.1 Nankaido megathrust earthquake. This structure also appears to represent a zone of high electrical conductivity which Kodaira et al. (2002) interpret as an overpressured fluid-rich layer. Contained fluids are inferred to be predominantly aqueous (including free water within pore/fracture space and bound water within hydrous minerals) with lesser CO_2 and hydrocarbons.

Stress heterogeneity within a subduction interface shear zone (SISZ)

Subduction mélange formations are typically characterized by relatively competent phacoids of sandstone, cherts, and metavolcanics set in a mud-rich matrix (Kimura et al. 2012). In deeper portions of the seismogenic zone ($T > 150$ °C) where ductile deformation mechanisms (e.g. solution transfer) come into play, progressive simple shear leads to the development of an oblique foliation along X – Y planar trajectories of the finite strain ellipsoid in the fine-grained mud matrix (Fig. 10), the degree of obliquity to the shear zone walls decreasing with increasing shear strain (Ramsay and Graham 1973). As noted by Bridgewater et al. (1973), the finite X stretching direction then ends up lying subparallel to the regional shortening direction. Where present, such foliation anisotropy may become a preferential failure plane for propagating earthquake ruptures.

Within mélange formations in the Shimanto Belt of SW Japan, Kimura et al. (2012) noted the predominance of quartz \pm calcite extension veins developed in sandstone phacoids, roughly orthogonal to their long axes. The stress state inside a phacoid is dominated by fibre stresses imposed by viscous drag along the boundaries of competent layers (Lloyd et al. 1982; Needham 1987) giving rise to ‘pinch and swell’ features (sometimes involving low-angle Riedel shears), boudinage, and extension fractures/veins developed orthogonal to the long axes of phacoids. Comparable systems of predominantly quartz extension veins disrupt competent phacoids in the Chrystalls Beach mélange of SE Otago, NZ, a mixed continuous–discontinuous shear zone developed in an accretionary setting of Triassic age (Fagereng 2011). However, as well as extension veins developed in the phacoids, innumerable, incrementally developed quartz (and, locally, calcite) slickenfibres veins with consistent shear sense are developed on shear surfaces lying subparallel to the flat-lying matrix foliation. Again, the extension veins are



predominantly orthogonal to phacoid long axes and near-perpendicular to the flat-lying foliation developed in the surrounding mud-rich matrix. Microstructural analyses demonstrate that the flat-lying slickenfibres and near-orthogonal extension veins in relatively competent sandstone phacoids were coeval, together forming a fault–fracture mesh accommodating brittle shearing along the foliation (Fagereng et al. 2010). It appears that because of the large rotational strains developed within a SISZ, stress states induced within extending phacoids are locally dominant and distinct from the far-field stress field driving thrust-shearing across the SISZ (Fig. 10).

Low-permeability seals within SISZ

For near-lithostatic overpressures to be developed and maintained within a SISZ, bulk permeability must average $<10^{-20}$ m², or an order of magnitude lower if the overpressures are contained by a thin (<1 km) caprock seal (Peacock et al. 2011). Among contributing factors to the development of such low permeabilities, the first is the likely presence of a high proportion of fine-grained silicic mudrock and the second, the active hydrothermal environment ($150 < T < 350$ °C) within at least the lower

half of the seismogenic SISZ. Under such conditions solution transfer will tend to reduce porosity and infills fractures with hydrothermal precipitates over short distance and time scales, contributing to silicification seals and adding cohesive strength (Rutter 1976; Kawabata et al. 2007; Rowe et al. 2009; Fisher and Brantley 2014). In addition, high strain shearing during progressive metamorphism will impose a foliation defined by aligned phyllosilicates oblique, but subparallel to the SISZ margins giving rise to permeability anisotropy with foliation-perpendicular permeability significantly lower than that parallel to foliation, thereby impeding vertical fluid transport. Formation of fault–fracture permeability during ongoing deformation competes with permeability reduction as a consequence of hydrothermal precipitation.

SISZ host seismogenic megathrusts which typically rupture at intervals of 100–1000 years, or so. Permeability within a SISZ thus varies with time, changing from extremely low values pre-failure to high localized values postfailure when high fracture permeability is expected within rupture zones with fractures predominantly aligned subparallel to foliation in the SISZ. Post-failure ‘seismogenic permeability’ may be in the range,

10^{-16} – 10^{-13} m² (Talwani et al. 2007), but will likewise be anisotropic with higher values subparallel to the foliation and the margins of the SISZ. These high postfailure permeabilities are, however, likely to be transitory diminishing rapidly through the aftershock period as a consequence of fracture healing and cementation in the active hydrothermal environment (cf. Bosl and Nur 2002).

A potentially important additional source of silica-saturated fluid comes from serpentinization of the forearc mantle (Hyndman et al. 2015), with fluid channelled along the SISZ to create low-permeability silicification caps along the SISZ hanging wall at depths of 25–40 km characterized by high V_p/V_s from silica enrichment (Audet and Bürgmann 2014). In combination with the effects of solution transfer within SISZ, silicification arising from serpentinization has multiple effects—restoring cohesive strength to existing fractures, reducing porosity, precipitating low-permeability seals, and promoting overpressuring in areas of fluid release.

Association with anomalous slip behaviour

Along northern portions of the Hikurangi subduction margin offshore from Gisborne, New Zealand, Bell et al. (2010) have demonstrated an association between low-dipping (0° – 9°) areas of the subduction interface at shallow depth (c. 10 ± 5 km) that are undergoing periodic slow-slip with anomalously high seismic reflectivity in regions where the interface is locally upwarped by subducting seamounts. The anomalous reflectivity is attributed to overpressured fluid-rich sediments. At depths of 25–25 km along the Tokai segment of the Nankai Trough subduction system, immediately northeast of the 1944 M_w 8.1 Tonankai megathrust rupture, Kodaira et al. (2004) find an association between the 60 km \times 60 km areal extent of a slow-slip event on the interface locally dipping c. 16° and a highly reflective portion of the plate interface directly overlying subducted oceanic crust with anomalously high Poisson's ratio denoting strong fluid overpressuring. The down-dip limit to seismogenic activity in the Nankai subduction system is defined by a belt of non-volcanic tremor [NVT—equivalent to episodic tremor and slip (ETS) in Cascadia] at depths of c. 35–45 km (Obara 2002). Very-low-frequency earthquakes with extremely low stress drops located in the Nankai accretionary prism are likewise attributed to rupturing of fluid-saturated rock under extreme overpressure (Ito and Obara 2006). A high-resolution study of this belt by Shelly et al. (2006) reveals a band of low-frequency earthquakes (LFEs) along the subduction interface dipping 10° NNW overlying a band of microearthquakes within the oceanic crust of the subducting lithosphere which, from its V_p/V_s signature, appears to be fluid-rich from metamorphic dewatering and highly overpressured.

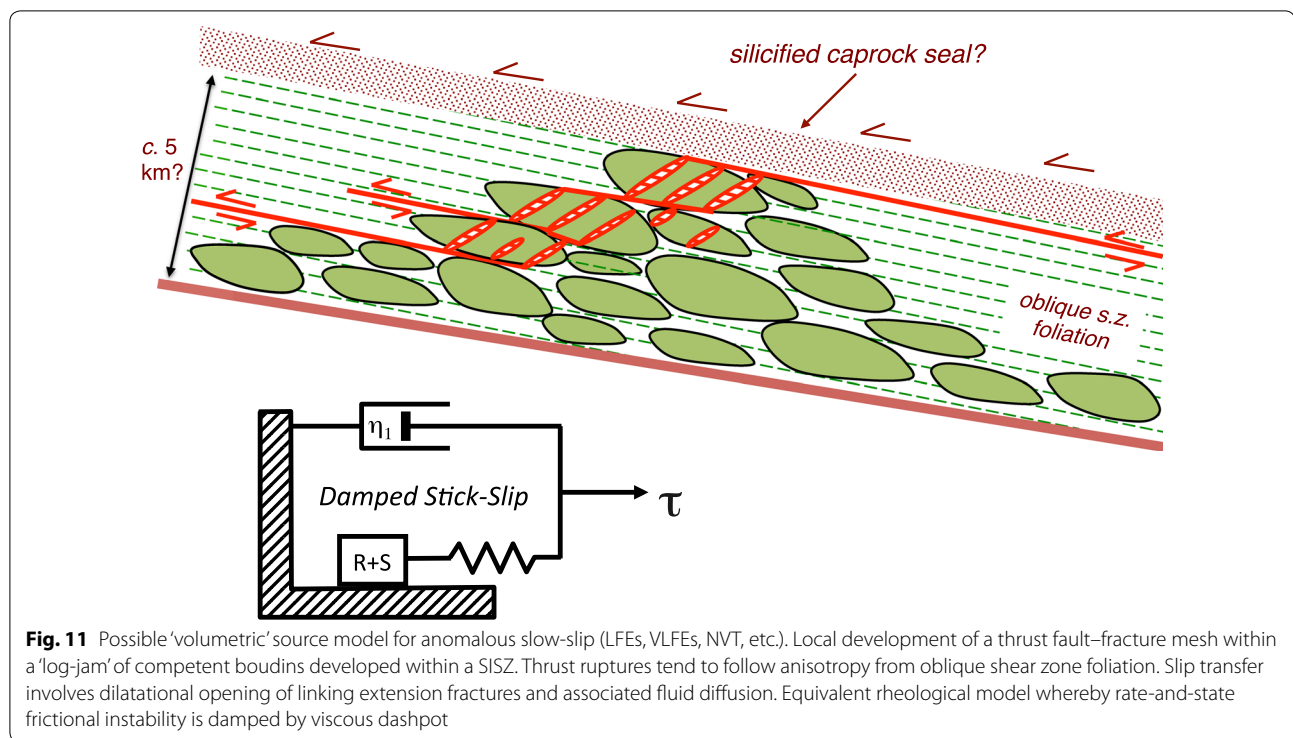
Discussion and conclusions

The hypothesis advanced here is that local attainment of the *tensile overpressure state* ($P_f > \sigma_3$) is associated with formation and activation of distributed fault–fracture meshes that are capable of giving rise to a variety of anomalous slow-slip phenomena (LFEs, VLFES, NVT, etc.). A great deal of circumstantial evidence supports this hypothesis, but further testing is clearly needed for full substantiation.

Geological and geophysical field evidence suggests that the *tensile overpressure state* (creating tensile overpressure compartments where $\sigma_3' = (\sigma_3 - P_f) < 0$, and hydraulic fracturing is widespread) is locally developed in both sub-greenschist and greenschist metamorphic assemblages. An association with active low-angle thrust faults (dips mostly $< 15^\circ$) in compressional regimes (including continental thrusts and subduction thrust interfaces) is sometimes evident from inferred geophysical characteristics (high seismic reflectivity, anomalously high V_p/V_s , and high electrical conductivity), suggesting that ~lithostatic levels of fluid overpressuring (i.e. $P_f \sim \sigma_c$) are locally achieved. In some instances, a relationship between potential tensile overpressure compartments and different varieties of anomalous slip phenomena (slow-slip events, LFEs, VLFES, NVT, etc.) is apparent.

Circumstances contributing to the development of distributed fault–fracture meshes in tensile overpressure compartments include: (1) varying competence within the rock mass (e.g. in a *mélange* formation) inducing diverse modes of brittle failure (Fagereng and Sibson 2010; Fagereng 2011; Kimura et al. 2012); (2) extensive solution transfer of silica and other hydrothermal materials following dissolution along foliation which serves to reduce existing porosity, helps form low-permeability seals promoting development of overpressure, and restores cohesion across existing fractures preventing shear localization (Kawabata et al. 2007; Rowe et al. 2009). For example, the intensely veined Rodeo Cove thrust zone at Marin Headlands within the Franciscan Complex of California has many of the hallmarks of a subduction fault–fracture mesh assemblage (Meneghini and Moore 2007).

Incremental shear displacement across fault–fracture meshes necessarily involves dilatation of extension fractures coupled to increments of shear displacement so that they have a tendency to act as viscous ‘dashpots’ slowing down slip transfer (Fig. 11). This allows a spectrum of time-dependent behaviour depending on the proportion of shear to extensional fractures, fluid viscosity, rate of overpressure generation, etc. Such structures may plausibly be responsible for the range of observed slow-slip behaviour including LFEs, VLFES, NVT (or ETS). Maintenance of near-lithostatic fluid overpressures



is precarious, and it is likely that fault–fracture meshes overpressured to near-lithostatic levels are extremely unstable. Loss of fluid from an overpressured mesh will cause frictional strengthening and a change in slip behaviour.

Acknowledgements

I thank the organizers and, in particular, Professor Yoshihisa Iio for making it possible for me to participate in the International Symposium 'Crustal Dynamics 2016: Unified Understanding of Geodynamics Processes at Different Time and Length Scales', held in Takayama City. I would also like to thank two anonymous reviewers for insightful and helpful criticism of this manuscript.

Publisher's Note

Springer Nature remains neutral with regard to jurisdictional claims in published maps and institutional affiliations.

Received: 8 April 2017 Accepted: 31 July 2017

Published online: 15 August 2017

References

- Abers GA (2005) Seismic low-velocity layer at the top of subducting slabs: observations, predictions, and systematics. *Phys Earth Planet Int* 149:7–29
- Anderson EM (1905) The dynamics of faulting. *Trans Edin Geol Soc* 8:387–402
- Audet P, Bürgmann R (2014) Possible control of subduction slow-earthquake periodicity by silica enrichment. *Nature* 510:389–392
- Badertscher NP, Burkhard M (2000) Brittle–ductile deformation in the Glarus thrust Lochseiten (LK) calc–mylonite. *Terra Nova* 12:281–288
- Baisch S, Weidler R, Vörös R, Wyborn D, DeGraaf L (2006) Induced seismicity during the stimulation of a geothermal HFR reservoir in the Cooper Basin (Australia). *Seismol Soc Am Bull* 96:2242–2256
- Baisch S, Vörös R, Weidler R, Wyborn D (2009) Investigation of fault mechanisms during geothermal reservoir stimulation experiments in the Cooper Basin (Australia). *Seismol Soc Am Bull* 99:148–158
- Baisch S, Rothert E, Stang H, Vörös R, Koch C, McMahon A (2015) Continued geothermal reservoir stimulation experiments in the Cooper Basin (Australia). *Seismol Soc Am Bull* 105:198–209. doi:10.1785/0120140208
- Bangs NL, McIntosh KD, Silver EA, Kluesner JW, Ranero CR (2015) Fluid accumulation along the Costa Rica subduction thrust and development of the seismogenic zone. *J Geophys Res* 120:67–86. doi:10.1002/2014JB01265
- Bell R, Sutherland R, Barker DHN, Henrys S, Bannister S, Wallace L, Beavan J (2010) Seismic reflection character of the Hikurangi subduction interface, New Zealand, in the region of the repeated Gisborne slow slip events. *Geophys J Int* 180:34–48
- Boer RH, Meyer FM, Robb LJ, Graney JR, Vennemann TW, Kesler SE (1995) Mesothermal-type mineralization in the Sabie–Pilgrim's Rest gold field, South Africa. *Econ Geol* 90:865–876
- Bosl WJ, Nur A (2002) Aftershocks and pore fluid diffusion following the 1992 Landers earthquake. *J Geophys Res* 107(B12):2366. doi:10.1029/2001JB000155
- Bridgewater D, Escher A, Watterson J (1973) Tectonic displacements and thermal activity in two contrasting Proterozoic mobile belts from Greenland. *Phil Trans R Soc Lond A* 273:513–533
- Byerlee JD (1978) Friction of rocks. *Pure Appl Geophys* 116:615–626
- Célérier B (2008) Seeking Anderson's faulting in seismicity: a centennial celebration. *Rev Geophys* 46:RG4001. doi:10.1029/2007RG000240
- Cox SF (2016) Injection-driven swarm seismicity and permeability enhancement: implications for the dynamics of hydrothermal ore systems in high fluid-flux overpressured faulting regimes—an invited paper. *Econ Geol* 111:559–587
- Dahlen FA (1990) Critical taper model of fold-and-thrust belts and accretionary wedges. *Ann Rev Earth Planet Sci* 18:55–99
- Eberhardt-Phillips D, Reyners M (1999) Plate interface properties in the northeast Hikurangi subduction zone, New Zealand, from converted seismic waves. *Geophys Res Lett* 26:2565–2568
- Etheridge MA (1983) Differential stress magnitudes during regional deformation and metamorphism: upper bound imposed by tensile fracturing. *Geology* 11:231–234

- Fagereng A (2011) Geology of the seismogenic subduction thrust interface. In: Fagereng A, Toy VG, Rowland JV (eds) *Geology of the earthquake source: a volume in honour of Rick Sibson*. Geological Society, London, Special Publications, vol 359, pp 55–76
- Fagereng A, Sibson RH (2010) Mélange rheology and seismic style. *Geology* 38:751–754
- Fagereng A, Remitti F, Sibson RH (2010) Shear veins observed within anisotropic fabric at high angles to the maximum compressive stress. *Nat Geosci* 3:482–485
- Ferrill DA, Morris AP (2003) Dilational normal faults. *J Struct Geol* 25:183–196
- Fisher DM, Brantley SL (2014) The role of silica redistribution in the evolution of slip instabilities along subduction interfaces: constraints from the Kodiak accretionary complex, Alaska. *J Struct Geol* 69:395–414
- Foxford KA, Nicholson R, Polya DA, Hebblethwaite RPB (2000) Extensional failure and hydraulic valving at Minas da Panasqueira, Portugal: evidence from spatial vein distributions, displacements and geometries. *J Struct Geol* 22:1065–1086
- Fuis GS, Ryberg T, Godfrey NJ, Okaya DA, Murphy JM (2001) Crustal structure and tectonics from the Los Angeles basin to the Mojave desert, southern California. *Geology* 29:15–18
- Harley M, Charlesworth EG (1992) Thrust-controlled gold mineralization at the Elandschoogte Mine, Sabie-Pilgrim's Rest goldfield, South Africa. *Miner Depos* 27:122–128
- Harley M, Charlesworth EG (1996) The role of fluid pressure in the formation of bedding-parallel thrust-hosted gold deposits, Sabie-Pilgrim's Rest goldfield, eastern Transvaal. *Precambrian Res* 79:125–140
- Hasegawa A, Yoshida K, Asano Y, Okada T, Iinuma T, Ito Y (2012) Change in stress field after the great Tohoku-oki earthquake. *Earth Planet Sci Lett* 355–356:231–243. doi:[10.1016/j.epsl.2012.08.042](https://doi.org/10.1016/j.epsl.2012.08.042)
- Herwegh M, Hürzeler J-P, Pfiffner OA, Schmid SM, Abart R, Ebert A (2008) The Glarus thrust: excursion guide and report of a field trip of the Swiss Tectonic Studies Group (Swiss Geological Society, 14–16/09/2006). *Swiss J Geosci* 101:323–340
- Holl H-G, Barton C (2015) Habanero field—structure and state of stress. In: *Proceedings of world geothermal congress 2015, Melbourne, Australia, 19–25 April 2015*
- Hubbert MK, Rubey WW (1959) Role of fluid pressure in the mechanics of overthrust faulting. *Geol Soc Am Bull* 70:115–166
- Hunt JM (1990) Generation and migration of petroleum from abnormally pressured fluid compartments. *Am Assoc Petrol Geol Bull* 74:1–12
- Hyndman RD (2007) The seismogenic zone of subduction thrust faults: what we know and what we don't know. In: Dixon TH, Moore JC (eds) *The seismogenic zone of subduction thrust faults*. Columbia University Press, New York, pp 15–40
- Hyndman RD, McCrory PA, Wech A, Kao H, Ague J (2015) Cascadia subducting plate fluids channelled to fore-arc mantle corner: ETS and silica deposition. *J Geophys Res* 120:4344–4358. doi:[10.1002/2015JB011920](https://doi.org/10.1002/2015JB011920)
- Ito Y, Obara K (2006) Dynamic deformation of the accretionary prism excites very low frequency earthquakes. *Geophys Res Lett* 33:L02311. doi:[10.1029/2005GL025270](https://doi.org/10.1029/2005GL025270)
- Jaeger JC, Cook NGW (1979) *Fundamentals of rock mechanics*, 3rd edn. Chapman & Hall, London, p 593
- Kawabata K, Tanaka H, Kimura G (2007) Mass transfer and pressure solution in deformed shale of accretionary complex: examples from the Shimanto Belt, southwestern Japan. *J Struct Geol* 29:697–711
- Kennedy LA, Logan JM (1997) The role of veining and dissolution in the evolution of fine-grained mylonites; the McConnell thrust, Alberta. *J Struct Geol* 19:785–797
- Kimura G, Yamaguchi A, Hojo M, Kitamura Y, Kameda J, Ujiie K, Hamada Y, Hamahashi M, Hina S (2012) Tectonic mélange as fault rock of subduction plate boundary. *Tectonophysics* 568–569:25–38
- Kodaira S, Kurashimo E, Park J-O, Takahashi N, Nakanishi A, Miura S, Iwasaki T, Hirata N, Ito K, Kaneda Y (2002) Structural factors controlling the rupture process of megathrust earthquakes at the Nankai trough seismogenic zone. *Geophys J Int* 149:815–835
- Kodaira S, Iidaka T, Kato A, Park J-O, Iwasaki T, Kaneda Y (2004) High pore fluid pressure may cause silent slip in the Nankai Trough. *Science* 304:1295–1298
- Kurtz RD, DeLaurier JM, Gupta JC (1990) The electrical conductivity distribution beneath Vancouver Island: a region of active plate subduction. *J Geophys Res* 95:10929–10946
- Lamb S (2006) Shear stresses on megathrusts: implications for mountain building behind subduction zones. *J Geophys Res* 111:B07401. doi:[10.1029/2011JB009133](https://doi.org/10.1029/2011JB009133)
- Lay T, Kanamori H, Ammon CJ, Koper KD, Hutko AR, Ye L, Yue H, Rushing TM (2012) Depth-varying rupture properties of subduction zone megathrust faults. *J Geophys Res* 117:B04311. doi:[10.1029/2011JB](https://doi.org/10.1029/2011JB)
- Lisle RJ, Orife TO, Arlegui L, Liesa C, Srivastava DC (2006) Favoured states of palaeostress in the Earth's crust: evidence from fault slip data. *J Struct Geol* 28:1051–1066
- Lloyd GE, Ferguson CC, Reading K (1982) A stress-transfer model for the development of extension fracture boudinage. *J Struct Geol* 4:355–372
- Lockner D (1995) Rock failure. In: Ahrens TJ (ed) *Rock physics and phase relations: a handbook of physical constants*, vol 3. AGU, Washington, Reference Shelf, pp 127–147
- McCaig AM, Wayne DM, Marshall JD, Banks D, Henderson I (1995) Isotopic and fluid inclusion studies of fluid movement along the Gavarnie Thrust, central Pyrenees: reaction fronts in carbonate mylonites. *Am J Sci* 295:309–343
- Meneghini F, Moore JC (2007) Deformation and hydrofracture in a subduction thrust at seismogenic depths: the Rodeo Cove thrust zone, Marin Headlands, California. *Geol Soc Am Bull* 119:174–183. doi:[10.1130/B25807.1](https://doi.org/10.1130/B25807.1)
- Needham DT (1987) Asymmetric extensional structures and their implications for the development of mélanges. *Geol Mag* 124:311–318
- Obara K (2002) Nonvolcanic deep tremor associated with subduction in southwest Japan. *Science* 296:1679–1681
- Pacheco JF, Sykes LR (1992) Seismic moment catalog of large shallow earthquakes, 1900–1989. *Seismol Soc Am Bull* 82:1306–1349
- Peacock SM (2004) Thermal structure and metamorphic evolution of subducting slabs. In: Eiler J (ed) *Inside the subduction factory*. Geophysics Mon, vol 138. AGU, Washington, pp 7–22
- Peacock SM, Christensen NI, Bostock MG, Audet A (2011) High pore pressures and porosity at 35 km depth in the Cascadia subduction zone. *Geology* 39:471–474. doi:[10.1130/G31649.1](https://doi.org/10.1130/G31649.1)
- Pfiffner OA (1986) Evolution of the North Alpine foreland basin in the Central Alps. In: Allen P, Homewood P (eds) *Foreland Basins*. Special Publications International Association of Sedimentology. Blackwells, Oxford, pp 219–228
- Ramsay JG (1980) The crack-seal mechanism of rock deformation. *Nature* 284:135–139
- Ramsay JG, Graham RH (1973) Strain variations in shear belts. *Can J Earth Sci* 7:786–813
- Robert F, Brown RA (1986) Archean gold-bearing quartz veins at the Sigma Mine, Abitibi greenstone belt, Quebec: part 1 Geologic relations and formation of the vein system. *Econ Geol* 81:578–592
- Rowe CD, Meneghini F, Moore JC (2009) Fluid-rich damage zone of an ancient out-of-sequence thrust, Kodiak Islands, Alaska. *Tectonics* 28:TC1006. doi:[10.1029/2007TC002126](https://doi.org/10.1029/2007TC002126)
- Rutter EH (1976) The kinetics of rock deformation by pressure solution. *Phil Trans R Soc Lond A283*:203–219
- Ryberg T, Fuis GS (1998) The San Gabriel Mountains bright reflective zone: possible evidence for young mid-crustal thrust faulting in southern California. *Tectonophysics* 286:31–46
- Saffer DM, Tobin HJ (2011) Hydrology and mechanics of subduction zone forearcs: fluid flow and pore pressure. *Annu Rev Earth Planet Sci* 39:157–186
- Schmid S (1975) The Glarus overthrust: field evidence and mechanical model. *Eclog Geol Hel* 68:247–280
- Secor DT (1965) Role of fluid pressure in jointing. *Am J Sci* 263:633–646
- Seno T (2009) Determination of the pore-fluid pressure ratio at seismogenic megathrusts in subduction zones: implications for strength of asperities and Andean-type mountain building. *J Geophys Res* 114:B05405. doi:[10.1029/2008JB005889](https://doi.org/10.1029/2008JB005889)
- Shelly DR, Beroza GC, Ide S, Nakamura S (2006) Low-frequency earthquakes in Shikoku, Japan, and their relationship to episodic tremor and slip. *Nature* 442:188–191
- Sibson RH (1985) A note on fault reactivation. *J Struct Geol* 7:751–754
- Sibson RH (1996) Structural permeability of fluid-driven fault–fracture meshes. *J Struct Geol* 18:1031–1042
- Sibson RH (2000) A brittle failure mode plot defining conditions for high-flux flow. *Econ Geol* 95:41–48

- Sibson RH (2003) Brittle failure controls on maximum sustainable overpressure. *Am Assoc Petrol Geol Bull* 87:901–908
- Sibson RH (2009) Rupturing in overpressured crust during compressional inversion—the case from NE Honshu, Japan. *Tectonophysics* 473:404–416
- Sibson RH (2014) Earthquake rupturing in fluid-overpressured crust: how common? *Pure Appl Geophys* 171:2867–2885
- Sibson RH, Scott J (1998) Stress/fault controls on the containment and release of overpressured fluids: examples from gold-quartz vein systems in Juneau, Alaska, Victoria, Australia, and Otago, New Zealand. *Ore Geol Rev* 13:293–306
- Song T-RA, Helmerger DV, Brudzinski MR, Clayton RW, Pérez-Campos X, Singh SK (2009) Subducting slab ultra-slow velocity layer coincident with silent earthquakes in southern Mexico. *Science* 324:502–506
- Soyer W, Unsworth M (2006) Deep electrical structure of the northern Cascadia (British Columbia, Canada) subduction zone: implications for the distribution of fluids. *Geology* 34:53–56. doi:[10.1130/G21951.1](https://doi.org/10.1130/G21951.1)
- Talwani P, Che L, Gahalaut K (2007) Seismogenic permeability, k_s . *J Geophys Res* 112:B07309. doi:[10.1029/2006JB004665](https://doi.org/10.1029/2006JB004665)
- Townend J, Zoback MD (2001) How faulting keeps the crust strong. *Geology* 28:399–402
- Tunks AJ, Selley D, Rogers JR, Brabham G (2004) Vein mineralization at Damang Gold Mine, Ghana: controls on mineralization. *J Struct Geol* 26:1257–1273
- Von Huene R, Scholl DW (1991) Concerning sediment subduction, subduction erosion, and the growth of continental crust. *Rev Geophys* 29:279–316
- Wang K, Suyehiro K (1999) How does plate coupling affect crustal stresses in Northeast and Southwest Japan. *Geophys Res Lett* 26:2307–2310
- Zoback ML (1992) First and second-order patterns of stress in the lithosphere: the World Stress Map project. *J Geophys Res* 97:11703–11728

Submit your manuscript to a SpringerOpen[®] journal and benefit from:

- Convenient online submission
- Rigorous peer review
- Open access: articles freely available online
- High visibility within the field
- Retaining the copyright to your article

Submit your next manuscript at ► [springeropen.com](https://www.springeropen.com)
